Journal of Coordination Chemistry

ISSN: 0095-8972 (Print) 1029-0389 (Online) Journal homepage: http://www.tandfonline.com/loi/gcoo20

Nickel(II) complexes with mono(imino)pyrrole ligands: preparation, structure and ethylene polymerization behavior

Biyun Su, Xudong Wang, Jiaxiang Wang & Xiaoteng Li

To cite this article: Biyun Su, Xudong Wang, Jiaxiang Wang & Xiaoteng Li (2015) Nickel(II) complexes with mono(imino)pyrrole ligands: preparation, structure and ethylene polymerization behavior, Journal of Coordination Chemistry, 68:23, 4212-4223, DOI: 10.1080/00958972.2015.1103371

To link to this article: http://dx.doi.org/10.1080/00958972.2015.1103371

Accepted author version posted online: 07 Oct 2015.
Published online: 03 Nov 2015.

Journal of Coordination Chemistry, 2015
Vol. 68, No. 23, 4212–4223, http://dx.doi.org/10.1080/00958972.2015.1103371

Nickel(II) complexes with mono(imino)pyrrole ligands: preparation, structure and ethylene polymerization behavior

BIYUN SU*†, XUDONG WANG†, JIAXIANG WANG‡ and XIAOTENG LI†

†The College of Chemistry and Chemical Engineering, Xi'an Shiyou University, Xi'an, China
‡Changzheng Engineering Co., Ltd, Lanzhou Branch, Lanzhou, China

(*Received 21 April 2015; accepted 17 August 2015*)

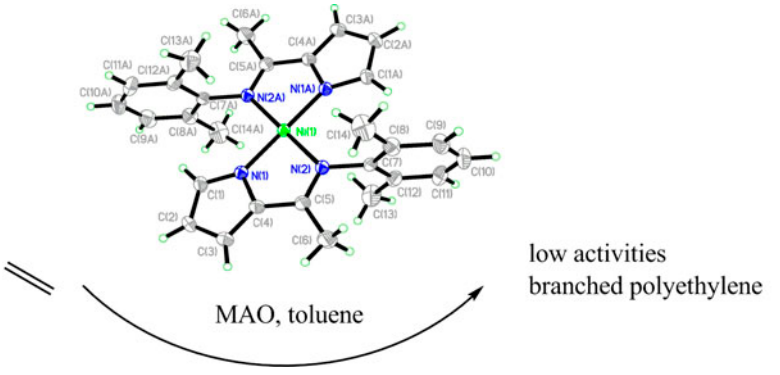

A series of unsymmetrical mono(imine)pyrroles (**L1–L3**) were synthesized by microwave irradiation from 2-acetylpyrrole and a series of dimethylanilines with two methyl groups at different positions on the aniline ring. A simplified synthetic method was initiated to prepare the corresponding nickel complexes NiL_2 (**1–3**) with direct condensation of mono(imine)pyrrole and nickel chloride. The compounds were determined using a suite of techniques (i.e. ^{1}H NMR, ^{13}C NMR, IR, EA, MS). **L1–L3** and **3** were further characterized by X-ray crystal diffraction. The structure of **3** showed that the ligand chelated to nickel with 2 : 1 M ratio, in spite of a 1 : 1 rate of charge. Application of **1–3** in ethylene polymerization indicated that mono(imino)pyrrole nickel complexes showed low activities. The polymerization reaction time and temperature, as well as the ligand structure, influenced the catalytic performance to some extent. Experimental data showed higher activity as $-CH_3$ on the aniline ring is closer to the imine group.

Keywords: Mono(imino)pyrrole; Nickel complex; Ethylene polymerization; Catalytic activity

1. Introduction

2,6-Bis(imino)pyridyl-Fe(II) and -Co(II) dihalides, activated by methylaluminoxane (MAO), were found to be effective catalysts for ethylene polymerization/oligomerization

*Corresponding author. Email: subiyun@xsyu.edu.cn

independently by Brookhart [1, 2] and Gibson [3, 4]. Bis(imino)pyridyl-metal catalysts have been an attractive research field because of their flexible structural modifications and complexation between ligand and metal, as well as outstanding catalytic performance. Studies have mainly concentrated on adjusting the structure of the ligand, usually using the following ways [5–8]: (1) introducing heteroatoms to the pyridine ring to get an N-based six-membered heterocyclic imino ligand, such as pyrimidine, pyrazine, and triazine ligands; (2) replacing the six-membered heterocycle with a five-membered heterocycle such as a pyrrole, thiophene, or furan ring; (3) modifying the imino substituent to get ligands with different side arms, such as carbazole or Pybox ligands [9]; or (4) changing the symmetric bis(imino) structure to an asymmetric structure [10–13]. For example, zirconium and titanium complexes bearing mono(imino)pyrrole ligands, reported by Fujita [14, 15] and Bochmann *et al*. [7], were demonstrated to be good catalysts for ethylene polymerization. Bochmann *et al*. [7] reported that 2,5-diacetylpyrrole reacted with 2,6-diisopropylaniline by a 1 : 1 M ratio could produce an asymmetric 2-aminopyrrole ligand. The corresponding iron, cobalt, and nickel complexes showed the catalytic activities to olefin polymerization. Cuesta *et al*. [16] studied the reactivities of mono(imino)pyrrole, mono(imino)thiophene, and mono(imino)furan with $[\{RuCl(\eta^6\text{-}p\text{-cymene})\}_2(\mu\text{-}Cl)_2]$, resulting in interesting structures.

Although a number of mono(imino)pyrrole ligands were developed, nearly all of the reported ligands bore H side arms [10–16]. We have expanded this work to mono(imino)pyrrole ligands with a $-CH_3$ side arm in order to have greater electronic and steric effects. The general method to synthesize imino pyrrole ligand has been to use conventional liquid-phase reactions under rigorous reaction conditions [15, 17]. To improve synthetic efficiency, we adopted microwave irradiation to promote the formation of mono(imino)pyrrole. The approach has proven to not only shorten the reaction time but also to improve the reaction yield and simplify the experiment process at the same time. The most used synthetic method for metal complexes has been treating the imino pyrrole ligand with a deprotonating reagent, then reacting it with metal salts to produce corresponding complexes [18]. Here, we tried to prepare NiL_2 (**L**: **L1–L3**; NiL_2: **1–3**) with the direct condensation of the mono(imine)pyrrole ligand and nickel chloride, which has proven to be feasible. The mono(imine)pyrrole ligands and nickel complexes were characterized by ^1H NMR, ^{13}C NMR, and IR spectroscopies, as well as EA and X-ray crystal diffraction. The nickel complexes were applied in the catalysis for ethylene polymerization, and the influences of conditions to the catalytic performance were studied.

2. Experimental

2.1. *General procedures and materials*

All experiments concerning air- and moisture-sensitive compounds were carried out under nitrogen using standard Schlenk techniques. Solvents were refluxed over an appropriate drying agent and distilled prior to use. C, H, and N analyses were performed with an HP-MOD 1106 microanalyzer. Fourier transform infrared (FT-IR) spectra were obtained with a Perkin-Elmer FTIR 2000 spectrometer. NMR spectra were recorded with a Bruker AVANCE III 500 spectrometer. Mass spectral (MS) analyses were performed with a Kratos AEIMS-50 instrument using the electron impact (EI) method. Microwave-assisted reactions were carried out in a Midea PJ 21B-A 800w (21L) microwave oven with a reflux condenser. 2-Acetylpyrrole, 2,4-dimethylaniline, 2,5-dimethylaniline, and 2,6-dimethylaniline were purchased from

Acros Co. and used as received. MAO in toluene (14 wt%) was from Albemarle Co. (USA). Polymerization-grade ethylene monomer, produced by Beijing Yanshan Petrochemical Co., was used without purification.

2.2. *Syntheses of ligands L1–L3 and nickel complexes 1–3*

2.2.1. 2-{1-[(2,4-Dimethylphenyl)imino]ethyl}pyrrole (L1). 2-Acetylpyrrole (152.2 mg, 1.395 mmol) and 2,4-dimethylaniline (301.1 mg, 2.485 mmol) were added to a 50-mL beaker with a 1 : 2 M ratio, then 1 mL of glacial acetic acid was added and blended well. The mixture was put in a microwave oven and irradiated at 600 W for 5 min. The obtained black crude product was purified by chromatographic column separation to afford a mass of white solid with a yield of 29.24% (0.2155 g). m.p. 396.8–398.4 K. IR (KBr): $\nu_{C=N}$ 1602.4 cm^{-1}. ^1H NMR (500 MHz, CD_2Cl_2): δ 9.64 (s, 1H, pyrrole N–H), 7.02 (t, 1H, benzene ring aromatic H), 6.95 (t, 1H, benzene ring aromatic H), 6.87 (t, 1H, pyrrole ring aromatic H), 6.63 (d, 1H, pyrrole ring aromatic H), 6.52 (d, 1H, benzene ring aromatic H), 6.23 (t, 1H, pyrrole ring aromatic H), 2.29 (s, 3H, –N=C(CH_3)–), 2.03 (d, 6H, phenyl–CH_3). $^{13}C\{^1H\}$ ($CDCl_3$): δ_C 16.46 (Me), 19.21 (o–Ph–Me), 19.92 (p–Ph–Me), 110.03 (C11), 117.97 (C10), 121.99 (C3, C2), 122.40 (C9, C8), 130.04 (C5, C6), 131.04 (C4), 137.21 (C1), 157.60 (C7) (Numbering scheme used for NMR labeling, see scheme 1). MS (EI): *m/z* 212 (M). Anal. Calcd for $C_{14}H_{16}N_2$ (%): C, 79.21; H, 7.60; N, 13.20. Found: C, 79.44; H, 7.03; N, 12.95.

2.2.2. 2-{1-[(2,5-Dimethylphenyl)imino]ethyl}pyrrole (L2). Using the same procedure as for the synthesis of **L1**, **L2**, a white solid was obtained with a yield of 27.29%. m.p. 396.8–398.4 K. IR (KBr): $\nu_{C=N}$ 1612.5 cm^{-1}. ^1H NMR (500 MHz, CD_2Cl_2): δ 9.89 (s, 1H, pyrrole N–H), 7.08 (t, 1H, benzene ring aromatic H), 6.82 (t, 1H, benzene ring aromatic H), 6.75(t, 1H, pyrrole ring aromatic H), 6.65 (d, 1H, pyrrole ring aromatic H), 6.49 (d, 1H, benzene ring aromatic H), 6.22 (t, 1H, pyrrole ring aromatic H), 2.30 (s, 3H, –N=C(CH_3)–), 2.04 (s, 6H, phenyl–CH_3). $^{13}C\{^1H\}$ ($CDCl_3$): δ_C 16.07 (o–Ph–Me), 17.46 (m–Ph–Me), 21.10 (Me), 109.61.

(C11), 112.09 (C4), 120.16 (C10), 121.9 (C2), 124.11 (C9), 125.10 (C8), 130.24 (C3), 132.46 (C6), 135.91 (C5), 149.34 (C7), 157.27 (C1) (Numbering scheme used for NMR labeling, see scheme 1). MS (EI): *m/z* 212 (M). Anal. Calcd for $C_{14}H_{16}N_2$ (%): C, 79.21; H, 7.60; N, 13.20. Found: C, 79.72; H, 7.13; N, 12.84.

2.2.3. 2-{1-[(2,6-Dimethylphenyl)imino]ethyl}pyrrole (L3). Using the same procedure as for the synthesis of **L1**, **L3**, a white solid was obtained with a yield of 15.92%. m.p.

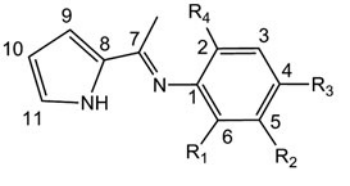

	R_1	R_2	R_3	R_4
L1	CH_3	H	CH_3	H
L2	H	CH_3	H	CH_3
L3	CH_3	H	H	CH_3

Scheme 1. Numbering scheme used for NMR labeling.

391.1–393.0 K. IR (KBr): $\nu_{C=N}$ 1610.2 cm^{-1}. ^1H NMR (500 MHz, CD_2Cl_2): δ 9.77 (s, 1H, pyrrole N–H), 7.04 (t, 2H, benzene ring aromatic H), 6.89 (t, 1H, benzene ring aromatic H), 6.81(t, 1H, pyrrole ring aromatic H), 6.65 (d, 1H, pyrrole ring aromatic H), 6.23 (t, 1H, pyrrole ring aromatic H), 2.01 (s, 6H, phenyl–CH_3), 1.93 (s, 3H, –N=C(CH_3)–). $^{13}C\{^1H\}$ ($CDCl_3$): δ_C 17.03 (o–Ph–Me), 17.05 (o–Ph–Me), 18.93 (Me), 113.02 (C11), 114.57 (C4), 120.16 (C10), 123.73 (C2), 126.33 (C9), 133.60 (C8), 134.45 (C3), 134.86 (C6), 137.08 (C5), 156.71 (C7), 158.02 (C1) (Numbering scheme used for NMR labeling, see scheme 1). MS (EI): *m/z* 212 (M). Anal. Calcd for $C_{14}H_{16}N_2$ (%): C, 79.21; H, 7.60; N, 13.20. Found: C, 79.55; H, 7.14; N, 13.09.

2.2.4. Bis{2-[(2,4-dimethylphenyl)ethyl]-1H-pyrrol-1-ido-k^{2}N,N′} nickel(II) (1). A mixed solution of $NiCl_2 \cdot 6H_2O$ (117 mg, 0.495 mmol) and 2-{1-[(2,4-dimethylphenyl) imino]ethyl}pyrrole (**L1**) (105 mg, 0.495 mmol) in ethanol (10 mL) was stirred at room temperature for 8 h. The solution was then concentrated to 4–6 mL, and a proper amount of deionized water was added. The mixture was allowed to stand for 1–2 h. The brick-red precipitate was filtered off and washed three times with deionized water and dried *in vacuo*. Yield: 86.6%. IR (KBr): $\nu_{C=N}$ 1589.4, 1586.7 cm^{-1}. ^1H NMR (500 MHz, CD_2Cl_2): δ 6.97–7.02 (m, 6H, benzene ring aromatic H), 6.49 (d, 2H, pyrrole ring aromatic H), 5.64 (d, 2H, pyrrole ring aromatic H), 4.68 (d, 2H, pyrrole ring aromatic H), 2.71 (s, 3H, –N=C(CH_3)–), 2.49 (s, 3H, –N=C(CH_3)–), 2.30 (d, 6H, phenyl–CH_3), 1.78 (d, 6H, phenyl–CH_3). Anal. Calcd for $C_{28}H_{30}N_4Ni$ (%): C, 69.88; H, 6.28; N, 11.64. Found: C, 69.39; H, 5.90; N, 11.32.

2.2.5. Bis{2-[(2,5-dimethylphenyl)ethyl]-1H-pyrrol-1-ido-k^{2}N,N′} nickel(II) (2). Using the same procedure as for the synthesis of **1**, **2**, a red solid was obtained with a yield of 76.4%. IR (KBr): $\nu_{C=N}$ 1605.7, 1600.2 cm^{-1}. ^1H NMR (500 MHz, CD_2Cl_2): δ 6.81–7.07 (m, 6H, benzene ring aromatic H), 6.51 (d, 2H, pyrrole ring aromatic H), 5.67 (s, 2H, pyrrole ring aromatic H), 4.70 (d, 2H, pyrrole ring aromatic H), 2.72 (s, 3H, phenyl–CH_3), 2.49 (s, 3H, phenyl–CH_3), 2.31 (d, 6H, phenyl–CH_3), 1.79 (d, 6H, –N=C(CH_3)–). Anal. Calcd for $C_{28}H_{30}N_4Ni$ (%): C, 69.88; H, 6.28; N, 11.64. Found: C, 69.76; H, 5.70; N, 11.24.

2.2.6. Bis{2-[(2,6-dimethylphenyl)ethyl]-1H-pyrrol-1-ido-k^{2}N,N′} nickel(II) (3). Using the same procedure as for the synthesis of **1**, **3**, a red solid was obtained with a yield of 88.9%. IR (KBr): $\nu_{C=N}$ 1598.4, 1588.6 cm^{-1}. ^1H NMR (500 MHz, CD_2Cl_2): δ 7.08–7.16 (m, 6H, benzene ring aromatic H), 6.50 (d, 2H, pyrrole ring aromatic H), 5.61 (m, 2H, pyrrole ring aromatic H), 4.45 (s, 2H, pyrrole ring aromatic H), 2.55 (s, 12H, phenyl–CH_3), 1.74 (s, 6H, –N=C(CH_3)–). Anal. Calcd for $C_{28}H_{30}N_4Ni$ (%): C, 69.88; H, 6.28; N, 11.64. Found: C, 70.02; H, 5.88; N, 11.20.

2.3. *X-ray single-crystal diffraction analyses of L1–L3 and 3*

All crystals of **L1**, **L2**, and **L3** were grown from an ethanol solution for one week. **L1** was a colorless tubular crystal; **L2** and **L3** were colorless needle-like crystals. The red-brown bulk crystal of **3** was obtained from layer by layer diffusion from methanol to the mixed

solvents of $HCCl_3$ and acetone ($V(HCCl_3) : V(acetone) = 1 : 1$) in three weeks. X-ray single-crystal diffraction data collection for **L1–L3** and **3** were collected at 296(2) K using a Bruker SMART 1000 diffractometer with graphite-monochromated Mo Kα radiation ($\lambda = 0.71073$ Å). The Smart program package was used to determine the unit cell parameters. A SADABS absorption correction was applied [19]. The structure was solved by direct methods and refined by full-matrix least-squares with anisotropic thermal parameters for non-hydrogen atoms. Hydrogens were placed at calculated positions and were included in the structure calculation without further refinement of the parameters. All calculations were performed using the SHELXS-97 program [20]. Crystal data and structure refinement for **L1–L3** and **3** are summarized in table 1.

2.4. *General procedure for ethylene polymerization*

10 μmol of the Ni complex was charged into a Schlenk tube. Air was eliminated from the Schlenk tube by three vacuum/nitrogen cycles. Then 50 mL of toluene and the desired volume of MAO/toluene solution (14%) were then added, and the mixture was stirred at 800 rpm for 10 min until the active catalytic species in toluene was available. A 100-mL stainless steel autoclave, equipped with a mechanical stirrer and a temperature controller, was evacuated by a vacuum pump and back-filled with N_2 three times and then filled with ethylene. The nickel active catalytic species was injected and the desired reaction temperature and pressure of ethylene were set. The mixture was vigorously stirred during the ethylene polymerization. The reaction solution was quenched by acidic ethanol and the precipitated polymer was filtered and washed several times with ethanol and then dried under vacuum at 50 °C for 24 h.

Table 1. Crystallographic data and structure refinement details for **L1–L3** and **3**.

Compound	**L1**	**L2**	**L3**	**3**
Empirical formula	$C_{14}H_{16}N_2$	$C_{14}H_{16}N_2$	$C_{14}H_{16}N_2$	$C_{28}H_{30}N_4Ni$
Formula weight	212.29	212.29	212.29	481.27
Temperature (*K*)	296(2)	296(2)	296(2)	296(2)
Crystal system	Monoclinic	Monoclinic	Monoclinic	Monoclinic
Space group	P2(1)/c	P2(1)/n	P2(1)/n	P2(1)/n
a (Å)	12.250	12.5894	8.1368	11.8117
b (Å)	10.358	7.3109	7.2398	7.3878
c (Å)	10.302	14.8425	21.542	15.169
α (°)	90	90	90	90
β (°)	107.022	113.118	96.989	109.444
γ (°)	90	90	90	90
Volume (Å^3)	1249.91	1256.43	1259.63	1248.23
Z, D_{Calcd} (Mg/m^3)	4, 1.128	4, 1.122	4, 1.119	2, 1.280
F(0 0 0)	456	456	456	508
Theta range (°)	1.74–25.09	1.81–25.98	2.80–25.10	1.91–25.10
Ref collection/unique	6156/2228	6471/2444	6092/2234	6012/2215
R(int)	0.1256	0.0208	0.0223	0.0271
Goodness-of-fit on F^2	1.089	1.009	1.044	1.050
R_1 [$I > 2\sigma(I)$][a]	0.1465	0.0455	0.0430	0.0339
wR_2 [$I > 2\sigma(I)$][b]	0.2972	0.1447	0.1200	0.0965
R_1 (all data)[a]	0.2540	0.0582	0.0527	0.0441
wR_2 (all data)[b]	0.3776	0.1634	0.1290	0.1154

[a] $R = \Sigma||F_o| - |F_c||/\Sigma|F_o|$.
[b] $wR = |\Sigma w(|F_o|^2 - |F_c|^2)|/\Sigma|w(F_o)^2|^{1/2}$.

3. Results and discussion

3.1. *Synthesis aspects*

The syntheses of ligands and the corresponding nickel complexes are shown in scheme 2. Initially, 2-acetylpyrrole reacts with a series of aniline derivatives by Schiff base condensation under microwave irradiation to get three novel mono(imino)pyrrole ligands (**L1–L3**). The reaction was inefficient under conventional liquid-phase condition, but proceeded easily with microwave irradiation. Using a microwave offers several advantages such as shorter reaction time, improved yield, and a simple reaction process. The solvent-free reaction is also in keeping with the green chemistry principle. All mono(imino)pyrrole ligands were reacted under mild microwave conditions (600 W) and the combination of the column chromatography and recrystallization method were used to obtain high purity.

Complexes **1–3** were synthesized by reacting Ni(II) chloride with a 1 : 1 stoichiometric amount of **L1–L3** in ethanol at room temperature. All complexes were isolated as air-stable solids in high purity. In the synthesis of amino pyrrole metal complexes, the weak acidities in pyrrole N–H were always thought to interfere with coordination, so the most commonly used method was to deprotonate the ligand using butyl lithium to produce a lithium complex [7], then reacted with a transition metal to get an imino pyrrole transition metal complex. Accidently, it was found that mono(imino)pyrrole nickel complex can be synthesized with the direct chelation of mono(imino)pyrrole ligand and Ni(II) chloride under very mild conditions (e.g. methanol solvent, room temperature). The process is of significance in terms of the procedure simplification and cost reduction.

3.2. *Molecular structures of L1–L3 and 3*

The molecular structures of **L1–L3** and **3** are shown in figures 1–4, respectively. Selected bond lengths and angles are listed in tables 2 and 3.

Figures 1–3 show that **L1**, **L2** [21], and **L3** have very similar mono(imino)pyrrole molecular structures. The ethyl group and imine are nearly coplanar with the pyrrole backbone

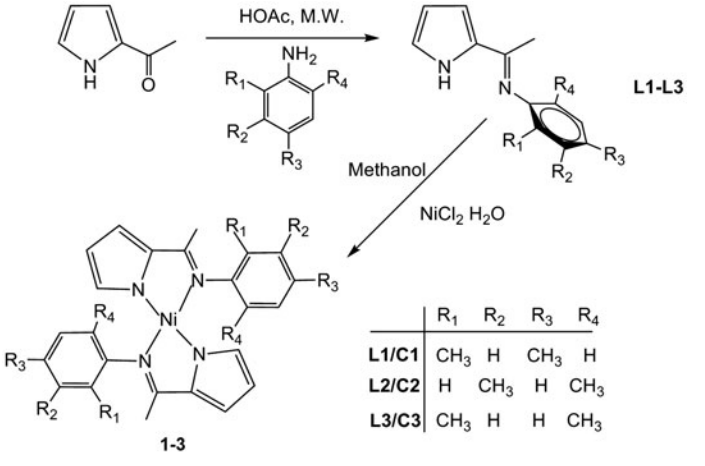

Scheme 2. Syntheses of **L1–L3** and **1–3**.

having a very small torsion angle of N(1)–C(4)–C(5)–N(2) (1.69° for **L1**, 3.22° for **L2**, 4.54° for **L3**). However, the benzene plane is oriented almost perpendicular to the pyrrole plane with a dihedral angle of 85.21° for **L1**, 81.26° for **L2**, and 77.24° for **L3**. Torsion angles decrease in the order of **L1**, **L2**, and **L3**, which indicates the closer the position of methyl to the imine group, the bigger the steric hindrance. Although the three ligands have very similar molecular structures, there are still some slight differences in bond lengths and bond angles. According to table 2, the lengths of C(4)–C(5) are 1.4569 Å for **L1**, 1.4542 Å for **L2**, and 1.4522 Å for **L3**, which show a decreasing length order of **L1**, **L2**, and **L3**. The lengths of N(2)–C(5) are 1.2858 Å for **L1**, 1.2862 Å for **L2**, and 1.2818 Å for **L3**, which show decreasing length order of **L2**, **L1**, and **L3**. The lengths of N(2)–C(7) are 1.4348 Å for **L1**, 1.4259 Å for **L2**, and 1.4274 Å for **L3**, which show a decreasing order of **L1**, **L3**, and **L2**. Generally, C(4)–C(5), N(2)–C(5) and N(2)–C(7) in all of these ligands are shorter than the normal carbon–carbon single bond (1.54 Å), carbon–nitrogen double bond (1.32 Å), and carbon–nitrogen single bond (1.47 Å). It is likely the conjugated system

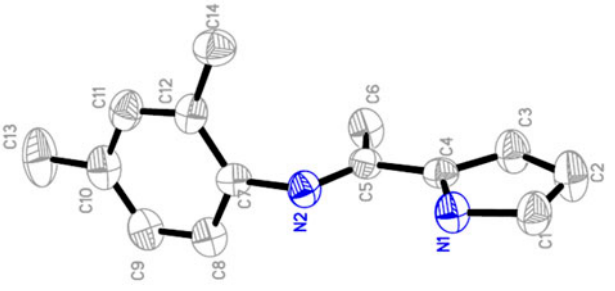

Figure 1. The molecular structure of **L1**.

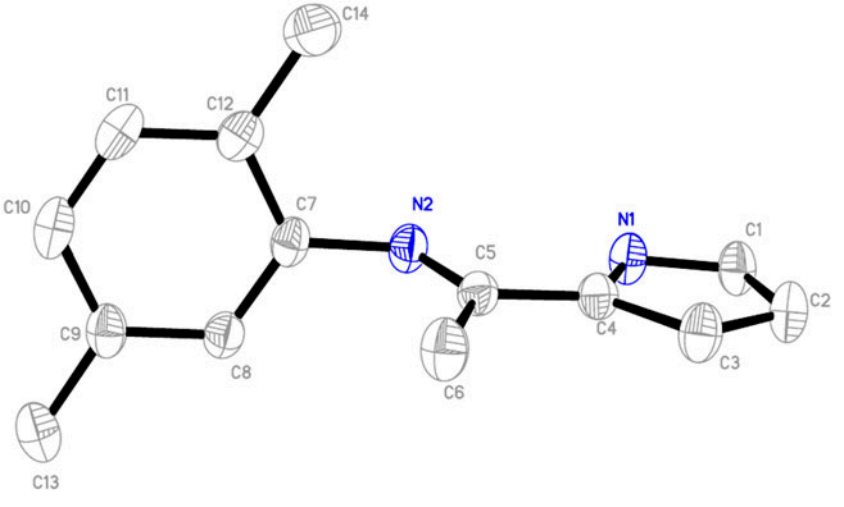

Figure 2. The molecular structure of **L2**.

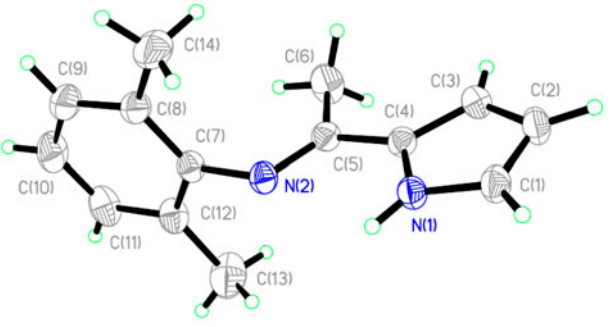

Figure 3. The molecular structure of **L3**.

Table 2. Selected bond lengths (Å) and angles (°) for **L1–L3**.

L1		**L2**		**L3**	
N1–C4	1.3665	N1–C4	1.3808	C4–N1	1.3732
N2–C5	1.2818	N2–C5	1.2858	N2–C5	1.2862
N2–C7	1.4274	N2–C7	1.4348	C7–N2	1.4259
C4–C5	1.4522	C4–C5	1.4569	C4–C5	1.4542
C5–C6	1.5022	C5–C6	1.4969	C5–C6	1.5052
N1–C4–C5	122.43	N1–C4–C5	122.96	N1–C4–C5	122.52
C3–C4–C5	130.57	C3–C4–C5	131.08	C3–C4–C5	130.71
C4–C5–C6	117.06	C4–C5–C6	116.85	C4–C5–C6	116.62
C4–C5–N2	118.56	C4–C5–N2	118.39	C4–C5–N2	119.39
C6–C5–N2	124.46	C6–C5–N2	124.75	C6–C5–N2	123.98
C5–N2–C7	118.56	C5–N2–C7	120.45	C5–N2–C7	120.10

formed by C=N group, pyrrole ring, and benzene ring causes the atoms to be more closely linked.

The series of mono(imino)pyrrole ligands also have a surprising similarity in hydrogen bonds. There are two classical intermolecular hydrogen bonds (N–H···N) and a pair of non-classical bonds (C–H···π) between the adjacent molecules of **L1**, **L2**, and **L3**. N–H···N hydrogen bonds are formed by H atoms from N–Hs on the pyrrole ring of one molecule and N atoms from the imide of another molecule. C–H···π bonds are formed by hydrogen from C–H on pyrrole ring of one molecule and benzene ring from the other molecule. By the four hydrogen bonds, each of the two molecules in **L1**, **L2**, and **L3** are linked into a center inversion symmetry dimer, and the unit of dimer further stacks from van der Waals force to produce the 3-D structure.

The molecular structure of **3** is shown in figure 4. The Ni(II) is coordinated by two inverted N,N′-bidentate mono(imino)pyrrole ligands using two imino and two pyrrolide nitrogens to form a four-coordinate geometry. Ni(II) is located in a crystallographic inversion center with the pyrrolide rings and the imine groups trans to each other. The sum of angles around the Ni(II) center is 360°, indicating square planar geometry. Two substituted phenyls on the imine N are almost vertical to the NiN_4 square plane with the same dihedral angles of 87.47° and are nearly parallel to each other due to the imposed inversion center. We note that the Ni–N_{imine} distances (1.9324 and 1.9322 Å) are substantially longer than the Ni–N_{pyr} bond (1.9162 Å), probably due to the anionic nature of the pyrrolide N and the

Table 3. Selected bond lengths (Å) and angles (°) for **3**.

C4–N1	1.3813	C4A–N1A	1.3813
C4–C5	1.4124	C4A–C5A	1.4124
C5–C6	1.4974	C5A–C6A	1.4974
N2–C5	1.3123	N2A–C5A	1.3123
C7–N2	1.4403	C7A–N2A	1.4403
N1–Ni1	1.9162	N1–Ni1–N2	83.00
N2–Ni1	1.9324	N1A–Ni1–N2A	83.00
N1A–Ni1	1.9162	N1A–Ni1–N2	97.00
N2A–Ni1	1.9322	N1–Ni1–N2A	97.00

steric hindrance of the phenyl ring substituents. However, all Ni–N bond lengths in **3** are shorter than the normal value for a typical Ni(II)–N bond (2.07 Å) [22]. This may indicate a stronger σ-donor character of N1 induced by the methyl (C6). The intramolecular C–H$\cdots\pi$ hydrogen bond, having the center inversion symmetry in **3**, strengthens the stability of the molecules. The intermolecular C–H$\cdots\pi$ hydrogen bond makes molecules assemble into 1-D supramolecular structures as zigzag chains. Comparison of crystal data of **L3** and **3** also highlights some differences in the structure. The first feature to note is that the **L3** bite angles in **3** (N_{imino}–Ni–N_{pyr}) are somewhat acute (83.01°), which decreases the complex angles N1–C4–C5 and N2–C5–C4 (114.62° and 115.42° in **3**, respectively) relative to those observed in **L3** (122.43° and 119.39°, respectively). At the same time, the C–N_{pyr}–C and C–N_{imino}–C angles decrease in the complex relative to free **L3**. The bond lengths appear to be significantly affected within the pyrrole ring. All C–C and C–N distances, apart from the C–C bond (C2–C3) opposite the N, appear to increase due to chelation to nickel. The C5=N2 double bond and N2–C7 bond are lengthened upon coordination, indicating the relatively strong π-back-donation from the Ni(II) center to the imine fragment.

3.3. *Application of nickel complexes in ethylene polymerization*

A series of ethylene polymerization experiments were carried out to investigate **1–3** performance. The influences of polymerization conditions were also studied, employing 10 μmol

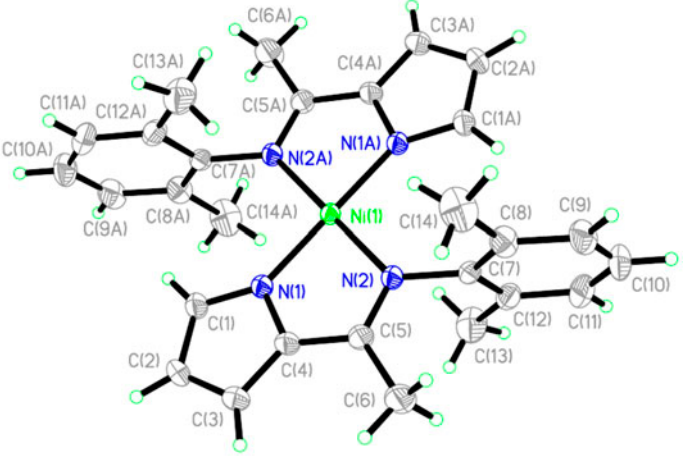

Figure 4. The molecular structure of **3**.

of catalyst and 50 mL of toluene as solvent, using MAO as cocatalyst (Al/Ni = 1000/1) under 1 atm of ethylene. The experimental data are listed in table 4.

3.3.1. Influence of polymerization time (comparing runs 1–5). Time significantly influences the catalytic activity for ethylene polymerization. Comparing runs 1–5, we can see that the catalytic activity continually went up with time. Complex **1** exhibited activity of 4.480 kg mol^{-1}(Ni) h^{-1} at 25 °C in 75 min, with the Al/Ni = 1000/1.

3.3.2. Influence of polymerization temperature (comparing runs 4, 6, 7 with 8, 9, 10 and 11, 12, 13). As previously reported [11], the catalytic systems are very sensitive to reaction temperature. By comparing runs 4, 6, 7 with 8, 9, 10 with 11, 12, 13, it was found that all the catalytic activities of **1**, **2**, and **3** increased from 25 to 50 °C and then decreased sharply as temperature continued to rise to 80 °C, which suggests the optimum temperature of the reaction is around 50 °C. A low temperature is unfavorable probably because it hinders the formation of active species, but too high of a temperature may cause a decrease in ethylene solubility and deactivation of the catalyst [23, 24]. The reason why the M_w of polymer at 80 °C is higher than that at 25 or 50 °C may be attributed to a higher temperature in favor of an increase in solubility of polymer in solvent or accelerating the chain growth rate, either of which may cause increase in the M_w of polymer [25, 26].

3.3.3. Influence of catalyst architecture (comparing run 4 with 6 and 7, 8 with 9 and 10, 11 with 12 and 13). Typically, a minor change in catalyst structure makes a significant difference in catalytic performance. Here, we mainly studied the influence of the dimethyl positions on the aniline ring. Comparing run 4 with 6 and 7, run 8 with 9 and 10, run 11 with 12 and 13, it can be clearly seen that **1**, **2**, and **3** exhibit different catalytic natures under the same reaction conditions.

Complex **3** showed the highest catalytic activities under each reaction condition. That means the methyl groups on the 2- and 6-positions of aniline in the complex structure promote increased catalytic activity. As far as M_w and M_w/M_n are concerned, **1** has higher

Table 4. Ethylene polymerization with nickel pre-catalysts/MAO.[a]

Run	Cat.	T (min)	Temp (°C)	Activity[b]	T_m[c] (°C)	M_w[d] (10^4 g mol^{-1})	M_w/M_n[d]
1	**1**	15	25	1.321	89.2	0.65	3.75
2	**1**	30	25	1.572	77.4	0.79	2.23
3	**1**	45	25	3.862	78.3	0.54	1.67
4	**1**	60	25	4.470	88.2	0.90	1.33
5	**1**	75	25	4.480	88.6	9.1	1.34
6	**2**	60	25	4.618	90.3	0.48	2.20
7	**3**	60	25	5.804	89.4	0.50	3.77
8	**1**	60	50	7.896	79.3	0.80	3.25
9	**2**	60	50	8.014	84.5	0.77	3.44
10	**3**	60	50	8.733	86.6	0.65	3.67
11	**1**	60	80	4.327	74.0	1.10	2.18
12	**2**	60	80	5.039	78.2	1.19	2.55
13	**3**	60	80	5.660	85.3	1.22	2.09

[a]Reaction conditions: 10 μmol Ni; MAO: Al/Ni = 1000, 1 atm ethylene; 50 mL toluene. MAO in toluene (3.7×10^{-3} mol mL^{-1}).
[b]kg mol^{-1}(Ni) h^{-1}.
[c]Determined by DSC.
[d]Determined by GPC.

molecular weights and narrower molecular weight distributions relative to **2** and **3**, especially at mild temperature. From the experimental data it may be concluded that the closer the $-CH_3$ on the aniline ring to the imine group, the more the electron density of imine will be influenced, which strengthens the coordination of the C=N to nickel. This may be the reason for the increased catalytic activity for **1**. ^{13}C NMR shows the polymer mainly contains short methyl branched chain, with branched degree of 65/1000, 77/1000, 79/1000 °C for **1**, **2**, and **3**, respectively, at 25 °C for 60 min. The branches in polymer chains are the main reason to cause low T_m [27].

4. Conclusion

A series of mono(imino)pyrrole ligands (**L1–L3**) and their corresponding Ni(II) complexes (**1–3**) have been synthesized. Ligands were synthesized using microwave irradiation instead of a conventional liquid-phase reaction. Direct coordination protonation strategy was adopted to generate the nickel complexes. Both innovations bring several advantages to the preparation of the mono(imino)pyrrole nickel catalysts, such as cost and time savings, operation simplification. The crystal structures of **L1–L3** and **3** were compared. Generally speaking, mono(imino)pyrrole nickel complexes showed low activities for ethylene polymerization. The polymerization reaction time and temperature and the ligand structure all influenced the catalytic performance to some extent. Experimental data show that the closer the $-CH_3$ on aniline ring is to the imine group the higher the activity.

Supplementary material

Crystallographic data for the structural analysis have been deposited with the Cambridge Crystallographic Data Center: CCDC No. 990761 for **L1**, CCDC No. 940614 for **L2**, CCDC No. 940616 for **L3**, CCDC No. 990769 for **C3**. Copies of these data may be obtained free of charge from the Director, CCDC, 12 Union Road, Cambridge CB2 1EZ, UK (E-mail: deposit@ccdc.cam.ac.uk; http://www.ccdc.cam.acuk).

Disclosure statement

No potential conflict of interest was reported by the authors.

Funding

This work was supported by the Scientific Research Plan Project of Shaanxi Education Department [grant number 12JK0620]; Science and Technology Research Program of Shaanxi Province [grant number 2013KJXX-33].

References

[1] B.L. Small, M. Brookhart. *J. Am. Chem. Soc.*, **120**, 7143 (1998).
[2] B.L. Small, M. Brookhart. U.S. Patent 6 150482, E.I. du Pont de Nemours and Company (2000).
[3] G.J.P. Britovsek, V.C. Gibson, B.S. Kimberley, P.J. Maddox, S.J. Mctavish, G.A. Solan, A.J.P. White, D.J. Williams. *Chem. Commun.*, 849 (1998).

[4] G.J.P. Britovsek, S. Mastroianni, G.A. Solan, S.P.D. Baugh, C. Redshaw, V.C. Gibson, A.J.P. White, D.J. Williams. *Chem. Eur. J.*, **6**, 2221 (2000).
[5] G.J.P. Britovsek, V.C. Gibson, O.D. Hoarau, S.K. Spitzmesser, A.J.P. White, D.J. Williams. *Inorg. Chem.*, **42**, 3454 (2003).
[6] L. Beaufort, F. Benvenuti, A.F. Noels. *J. Mol. Catal. A: Chem.*, **260**, 210 (2006).
[7] D.M. Dawson, D.A. Walker, M. Thornton-Pett, M. Bochmann. *J. Chem. Soc., Dalton Trans.*, 459 (2000).
[8] V.C. Gibson, S.K. Spitzmesser, A.J.P. White, D.J. Williams. *Dalton Trans.*, **13**, 2718 (2003).
[9] K. Nomura, W. Sidokmai, Y. Imanishi. *Bull. Chem. Soc. Jpn.*, **73**, 599 (2000).
[10] B.Y. Su, J.S. Zhao, Q.C. Gao. *Chin. J. Chem.*, **25**, 121 (2007).
[11] B.Y. Su, J.S. Zhao. *Polyhedron*, **25**, 3289 (2006).
[12] B.Y. Su, G.X. Feng. *Polym. Int.*, **59**, 1058 (2010).
[13] B. Su, J. Zhao, Q. Zhang, W. Qin. *Polym. Int.*, **58**, 1051 (2009).
[14] Y. Yoshida, S. Matsui, Y. Takagi, M. Mitani, M. Nitabaru, T. Nakano, H. Tanaka, T. Fujita. *Chem. Lett.*, **29**, 1270 (2000).
[15] Y. Yoshida, S. Matsui, Y. Takagi, M. Mitani, T. Nakano, H. Tanaka, N. Kashiwa, T. Fujita. *Organometallics*, **20**, 4793 (2001).
[16] L. Cuesta, T. Soler, E.P. Urriolabeitia. *Chem. Eur. J.*, **18**, 15178 (2012).
[17] S.A. Carabineiro, L.C. Silva, P.T. Gomes, L.C.J. Pereira, L.F. Veiros, S.I. Pascu, M.T. Duarte, S. Namorado, R.T. Henriques. *Inorg. Chem.*, **46**, 6880 (2007).
[18] K. Tenza, M.J. Hanton, A.M.Z. Slawin. *Organometallics*, **28**, 4852 (2009).
[19] G.M. Sheldrick. *SADABS, Program for Bruker Area Detector Absorption Correction*, University of Göttingen, Göttingen, Germany (1997).
[20] (a) G.M. Sheldrick. *SHELXS-97, Programs for Solution of Crystal Structure*, University of Göttingen, Germany (1997); (b) G.M. Sheldrick. *SHELXL-97, Programs of Refinement for Crystal Structure*, University of Göttingen, Germany (1997).
[21] B.Y. Su, W.L. Qin, J.X. Wang. *Acta Crystallogr. E*, **68**, o3008 (2012).
[22] A.G. Orpen, L. Brammer, F.H. Allen, O. Kennard, D.G. Watson, R. Taylor. *J. Chem. Soc., Dalton Trans.*, S1 (1989).
[23] M. Atiqullah, H. Hammawa, H. Hamid. *Eur. Polym. J.*, **34**, 1511 (1998).
[24] P.G.T. Fogg, W. Gerrard. *Solubility of Gases in Liquids*, Wiley, Chichester (1991).
[25] H.B. Gu, J.M. He, J. Hu, Y.D. Huang. *Mater. Sci. Technol.*, **18**, 108 (2010).
[26] B.Y. Jiang, H.G. Ji, B. Liao, H.L. Liu, H. Pang. *Fine Chem.*, **28**, 1004 (2011).
[27] J.Y. Ai, F.M. Zhu, S.A. Lin. *Polym. Mater. Sci. Eng.*, **21**, 94 (2005).